Assessing the equatorial long-wave approximation: asymptotics and observational data analysis (Supplementary Material)

by H. Reed Ogrosky and Samuel N. Stechmann

1. Kelvin and MRG waves

The analysis of section 6 is repeated here for the ϕ_0 and ϕ_1 components of equation (5.2) from the main text corresponding to the Kelvin, MRG, and EIG_0 waves.

a. Definition of wave variables

1) Kelvin wave

The ϕ_0 component of (5.2) is a single PDE governing a Kelvin wave,

$$\partial_t r_0 + \partial_x r_0 = 0. \tag{S1}$$

2) MRG and EIG_0 waves

The ϕ_1 component of (5.2) is a system of two coupled PDEs governing an MRG and EIG_0 wave,

$$\partial_t r_1 + \partial_x r_1 - v_0 = 0, \tag{S2a}$$

$$\partial_t v_0 + r_1 = 0. \tag{S2b}$$

Each of the variables in (S2) can be expressed as a superposition of plane-wave ansatzes

$$\hat{r}_1(k,\omega)e^{i(kx-\omega t)}, \qquad \hat{v}_0(k,\omega)e^{i(kx-\omega t)}; \tag{S3}$$

substituting (S3) into (S2) gives

$$\begin{bmatrix} i(k-\omega) & -1 \\ 1 & -i\omega \end{bmatrix} \begin{pmatrix} \hat{r}_1 \\ \hat{v}_0 \end{pmatrix} = \begin{pmatrix} 0 \\ 0 \end{pmatrix}. \tag{S4}$$

We are interested in finding the eigenmodes of (S4); its characteristic equation is

$$\omega^2 - k\omega - 1 = 0. \tag{S5}$$

There are two solutions, ω_j, for $j \in \{MRG, EIG_0\}$ to (S5). Each eigenvalue ω_j for $j \in \{MRG, EIG_0\}$ is associated with an eigenvector of the form

$$\vec{e}_{j0} = \left(-\frac{i}{k-\omega_j}, \quad 1\right)^T. \tag{S6}$$

The resulting eigenvectors are shown in Fig. S1 after normalization.

The degree to which the spatial structure of each of these two waves is seen in reanalysis data can be calculated by the projection technique described in section 6. Using this approach, the Fourier coefficients of the MRG and EIG_0 wave structures are defined as

$$\widehat{MRG}(k) = \vec{e}^{\dagger}_{MRG}(k) \begin{pmatrix} \hat{r}_1(k) \\ \hat{v}_0(k) \end{pmatrix}, \qquad \widehat{EIG}_0(k) = \vec{e}^{\dagger}_{EIG_0}(k) \begin{pmatrix} \hat{r}_1(k) \\ \hat{v}_0(k) \end{pmatrix}, \tag{S7}$$

respectively, where crosses denote the conjugate transpose. This spectral data may then be transformed back into physical space through an inverse Fourier transform.

b. Long-wave theory with wave variables

1) Kelvin wave

The Kelvin wave is unaffected by the long-wave approximation.

2) MRG AND EIG$_0$ WAVES

Projecting (5.7), i.e. with $\delta \ll 1$, onto ϕ_1 results in two coupled PDEs,

$$\partial_t r_1 + \partial_x r_1 - v_0' = 0, \tag{S8a}$$

$$\delta^2 \partial_t v_0' + r_1 = 0; \tag{S8b}$$

In the limit of small δ, the system (S8) can be expressed as an eigenvalue problem (written here in terms of $\hat{v}_0 = \delta \hat{v}_0'$),

$$\begin{bmatrix} i\delta(k-\omega) & -1 \\ 1 & -i\delta\omega \end{bmatrix} \begin{pmatrix} \hat{r}_1 \\ \hat{v}_0 \end{pmatrix} = \begin{pmatrix} 0 \\ 0 \end{pmatrix}. \tag{S9}$$

We are interested in finding the eigenmodes of (S9); its characteristic equation is

$$\delta^2\omega^2 - \delta^2 k\omega - 1 = 0. \tag{S10}$$

There are again two solutions, ω_j, for $j \in \{MRG, EIG_0\}$ to (S10), but in the limit $\delta \to 0$ both of these roots are singular. Each eigenvalue ω_j is associated with an eigenvector of the form

$$\vec{e}_{j0} = \left(-\frac{i}{k-\omega_j}, \quad \delta \right)^T. \tag{S11}$$

In the long-wave limit, approximate eigenvalues may be found by expanding in powers of δ,

$$\omega_{MRG} = -\delta^{-1} + O(1), \tag{S12a}$$

$$\omega_{EIG_0} = \delta^{-1} + O(1), \tag{S12b}$$

After a phase shift so that the r_1 component is positive and real, the normalized long-wave eigenvectors are, to leading order in δ, given by

$$\text{MRG}: \quad \vec{e}_{MRG} = \left(\frac{1}{\sqrt{2}}, \quad -\frac{i}{\sqrt{2}} \right)^T, \tag{S13a}$$

$$\text{EIG}_0: \quad \vec{e}_{EIG_0} = \left(\frac{1}{\sqrt{2}}, \quad \frac{i}{\sqrt{2}} \right)^T. \tag{S13b}$$

Note that the structure of these 'long-wave' eigenvectors is independent of k.

c. Observational data analysis

1) Kelvin wave

A Hovmoller plot of the Kelvin wave structure isolated in reanalysis data is shown in Fig. S2(a) for the one year period 1 July 2009 through 30 June 2010. Note the abundance of information propagating rapidly to the east, reminiscent of Kelvin waves. The power spectrum of the Kelvin wave structure is shown in the main text in Fig. 18(a).

2) MRG and EIG_0 waves

Fig. S2(b-c) shows the non-long-wave MRG and EIG_0 wave structures isolated in reanalysis data. The MRG wave exhibits the strongest activity between 180 and 90W, similar to the location of highest activity in the meridional winds v_0 (see Fig. 4b in the main text). This can be anticipated in light of the MRG wave being comprised almost entirely of v_0 at moderate to high wavenumbers, as in Fig. S1(a). Note also the large discrepancy between the MRG and EIG_0 structures in amplitude: the EIG_0 wave contains very little power at all frequencies and wavenumbers, while the MRG wave contains significant power at moderate wavenumbers. Both waves contain very little low-wavenumber information. These figures demonstrate that reanalysis data projects weakly onto the MRG and EIG_0 waves over spatial and temporal scales where the long-wave approximation holds.

LIST OF FIGURES

Fig. S1. Eigenvector components of the (a) *MRG* and (b) EIG_0 wave structures. 6

Fig. S2. Hovmoller plot of (a) Kelvin, (b) *MRG*, and (c) EIG_0 anomalies from a seasonal cycle. Time period shown is 1 July 2009 through 30 June 2010. 7

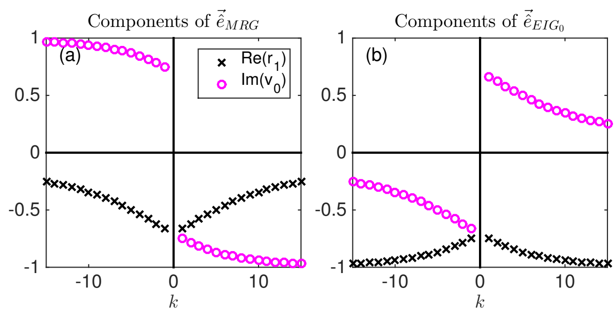

FIG. S1. Eigenvector components of the (a) *MRG* and (b) EIG_0 wave structures.

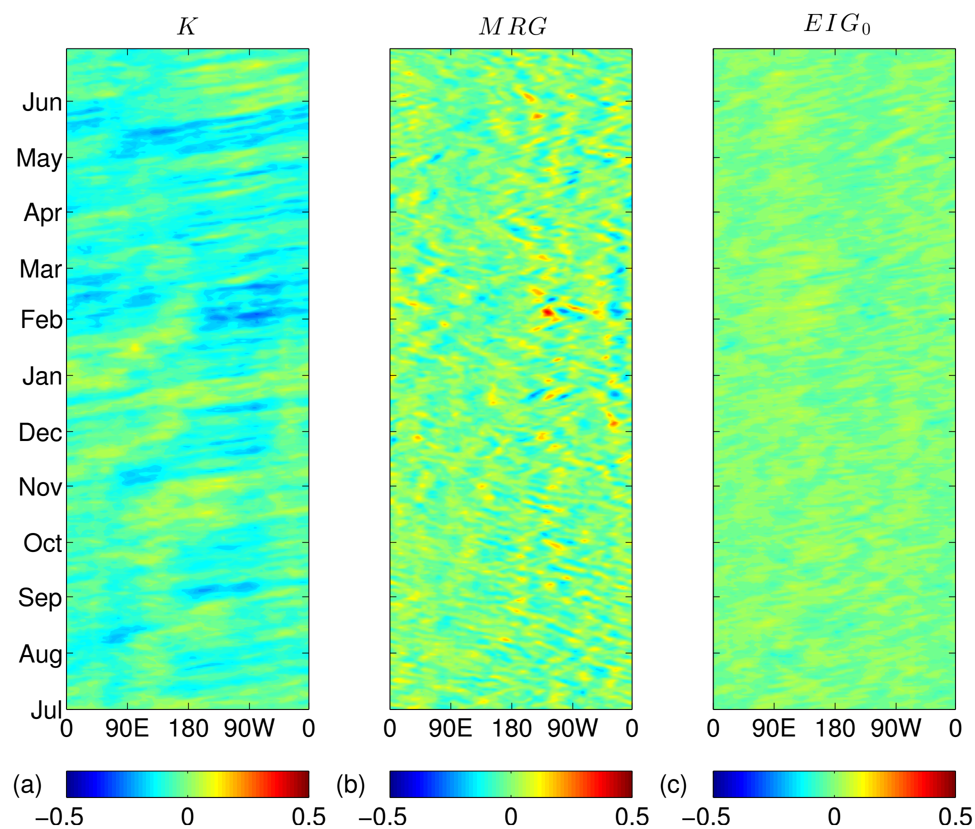

FIG. S2. Hovmoller plot of (a) Kelvin, (b) MRG, and (c) EIG_0 anomalies from a seasonal cycle. Time period shown is 1 July 2009 through 30 June 2010.